Unmanned marsupial sea–air system for object recovery

Nikola Mišković, Stjepan Bogdan, Đula Nađ, Filip Mandić, Matko Orsag and Tomislav Haus

Abstract— **This paper presents preliminary results obtained from a cooperative heterogeneous system consisting of an unmanned surface marine vehicle (USV) and an unmanned aerial vehicle (UAV). The envisioned scenario for this marsupial system is unmanned recovery of objects floating at the sea surface. The specific mission that is addressed in this paper includes the following phases: *coarse approach* where the USV approaches the object area using navigation filter based on GPS measurements; *fine approach* where the UAV tracking the USV sends relative distances between the USV and the object which is visible in the UAV's field of view; and *tugging* where the USV takes the object to safety after the initial contact has been achieved. The paper describes the ROS–based control architecture, presents simulation results, and addresses control issues related to obtaining measurements from two sources with different variances.**

I. INTRODUCTION

The term marsupial robotics, conveniently coined after mammals that carry their young in a pouch, was defined by Murphy et al. in [8] as a collection of mobile robots where one or more robots are at least temporarily physically dependent on another for directives, transport, power, and communication. In general, a marsupial team consists of a mother robot that hosts one or more dependent daughter robots. Marsupial teams are described in terms of what roles the mother holds: courier, messenger, manager, and coach, [8]. As a *courier*, the mother carries the daughter platforms and in that way increases their battery life, range of operation and processing power. The *messenger* role is fulfilled by routing data between the daughters and/or to the base station, while the *manager* role is accomplished by coordinating the team in a centralized way. The *coaching* role, the most interesting one for the results presented in this paper, is to act as an external, global point of view for other team members. However, it should be stated that these roles need not be defined only as the mother's roles. In a specific case of a sea–air cooperative heterogeneous system, comprising an unmanned surface marine vehicle (USV) and an unmanned aerial vehicle (UAV), the USV can be considered the mother since in carries the UAV to a desired position. However, the daughter UAV can serve as a messenger, routing data from the USV to the ground base station; the manager, coordinating the mother's motion; and a coach, providing a global birds–eye view of the situation for the mother.

The work described in this paper has been supported by the University of Zagreb as a short term financial support under the contract number 2013–ZUID–19.

The authors are with the University of Zagreb, Faculty of Electrical Engineering and Computing, Department of Control and Computer Engineering, Unska 3, Zagreb, Croatia nikola.miskovic at fer.hr

The majority of heterogeneous robotic systems reported in literature combine ground and aerial vehicles. The reason for this, most probably, lies in challenging logistics required to deploy sea/aerial systems, and great risk of destruction due to unfriendly environment. However, there is an increasing number of systems that include the maritime robotic component. The sea robot-assisted inspection (Sea–RAI) marsupial robot team is the first manportable USV that hosts a UAV, [5]. It is designed for inspecting littoral environments for military, environmental, and disaster–response applications. The results reported in [5] demonstrate the system functionality but they do not address autonomy nor cooperative aspects of the system. The SPAWAR system comprising a jet ski-based platform and an UAV, deploys the latter when needed for inspection purposes, [4]. The SPAWAR system does not appear to be implemented. A system developed by NATO–CMRE and UNIZG–FER for mine–countermeasure purposes consists of an autonomous surface catamaran and small dispensable autonomous underwater vehicle (AUV) that serves as an extended arm for close inspection of suspicious underwater objects. This heterogeneous system demonstrated full cooperative abilities where the surface vehicles navigates the AUV within the sonar image via acoustic link, [6].

This paper deals with a cooperative heterogeneous robotic system consisting of an autonomous surface marine platform and an unmanned aerial vehicle. The main objective of the system is to perform unmanned object recovery from the sea surface. The aspect that we are focusing on in this paper is the overall control strategy, and description of the cooperative nature of the system. Specifically, in the envisioned scenario, the daughter UAV (quadrotor) tracks the mother USV and sends the relative distance between the USV and the object of interest in order to *i)* ensure precise contact with the object and *ii)* tug the object to safety.

Mobile robots that will be used in real–life experiments are available from two groups at the University of Zagreb Faculty of Electrical Engineering and Computing: Laboratory for robotics and intelligent control systems - LARICS (unmanned aerial vehicles), and Laboratory for Underwater Systems and Technologies - LABUST (unmanned surface marine vehicles). The **unmanned surface vehicle (USV)** is an overactuated platform with 4 thrusters forming the "X" configuration that enables motion in the horizontal plane under any orientation. The platform has been developed at LABUST and the current version is 0.35m high, 0.707m wide and long. The platform was primarily developed for the purpose of diver tracking, [7].

Due to its simple mechanical design and open-source soft-

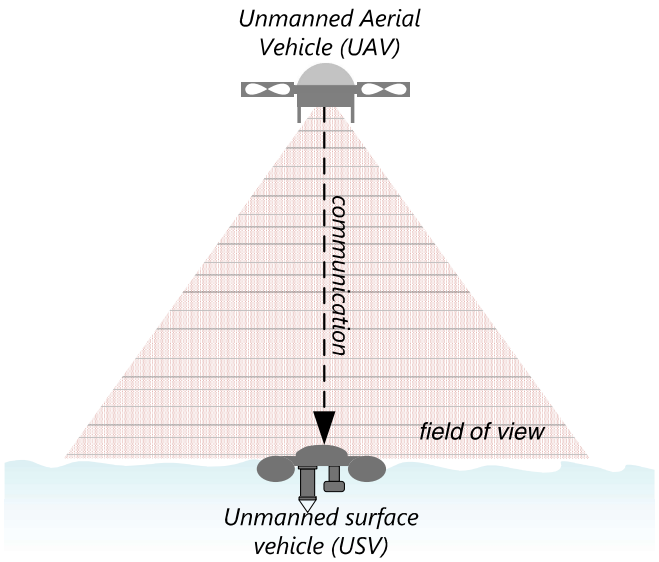

Fig. 1. The marsupial sea–air robotic system.

ware, **unmanned aerial vehicle (UAV)** ArduCopter Quad, from jDrones company, is one of the most popular aerial platforms with 4 propellers. Electronics, designed around Arduino processor, comprise complete set of sensors and features - 6 Degree of Freedom IMU stabilized control, gyro stabilized flight mode enabling acrobatics, magnetometer for heading determination, barometer for altitude hold, IR sensor integration for obstacle avoidance, and sonar sensor for automated takeoff and landing capability. This vehicle has recently been used to test hybrid adaptive control for aerial manipulation, [9].

The paper is structured as follows. Section II describes the full scenario of operation, from the USV and UAV perspectives. Mathematical models required to understand the control aspect of the system are given in Section III while the overall control structure is described in Section IV. Section V gives simulation results while Section VI concludes the paper.

II. Scenario description

The addressed marsupial system consists of an unmanned surface marine vehicle (USV) and an accompanying unmanned aerial vehicle (UAV) as it is shown in Fig. 1. The envisioned scenario for this marsupial system is unmanned recovery of objects floating at the sea surface. Specifically, we want to address the issue of recovery and neutralization of unexploded underwater ordnance (UxO) which is an extremely dangerous and destructive activity since an underwater explosion has a destruction radius much higher in comparison to the one on land. In the proposed scenario, we assume that the UxO has been successfully brought to surface by, for example, attaching a self–inflatable balloon to the underwater object and activating it remotely from a safe distance. Once the object has surfaced, and its position is known, the proposed marsupial system is launched. While the USV is navigating to the UxO area, the UAV is hovering above the USV, providing a bird's–eye view of the situation. Once the UAV notices the object to be recovered, it initiates the transmission of the relative distance between the USV and the object. This data is then used by the USV to fine navigate close to the object in order to be able to tug it to the area where the UxO can be neutralized.

In this paper, we will focus on the part of the scenario where the USV navigates to the object first by using available onboard navigation suite (GPS), and then by using more precise information provided by the UAV on the relative distance between the USV and the object. With this specific set of tasks, the following states from the point of view of the USV are addressed:

I. **Coarse approach.** In this mission state, the USV has to perform the line following manoeuvre while keeping such orientation to enable final grasping contact at a predefined point on the USV (between the two lever arms). From the control perspective, the USV has to follow a line to the object while maintaining a predefined heading (fully actuated line following). This manoeuvre is executed while the USV is at a distance from the object, i.e. while only GPS and compass data are available for navigation.

II. **Fine approach.** This state is initiated once the UAV, that is dynamically positioned above the USV, recognizes the object of interest within its field of view. The UAV then sends the information about the relative distance to the USV, and the USV positions itself to the object in such a way to enable the final contact, i.e. grasping between the two lever arms. From the control perspective, the USV, at this stage, has to perform dynamic positioning while keeping the orientation to the object, by using the data from the UAV. This manoeuvre is executed while the USV is close to the object and only UAV provided measurements and compass are used for navigation.

III. **Tugging.** Once the contact with the object is made, the platform has to tug the object to a predefined position, without loosing the object from between the lever arms. This requires a tugging manoeuvre with smooth heading change that will ensure contact with the object. From the control perspective, the USV has to perform a line following manoeuvre while keeping the heading always in the direction of the object (underactuated line following, [2]). During this state, GPS and compass measurements are used for navigation while the UAV monitors that the object has not left the contact point with the USV.

While the USV is performing the above mentioned activities, the UAV is simultaneously performing the following set of tasks:

I. **USV following.** In the spirit of marsupialism, the UAV is constantly tracking the UAV based on the processed images from the bird's-eye view. From the control perspective, UAV is performing the tracking algorithm

while simultaneously keeping a constant altitude. The only sensor that the UAV is equipped with is a camera and all the navigation relative to the USV is provided through the camera imagery.

II. **Object detection.** Since the UAV has a broader image of the USV surroundings, it is in charge of detecting the object that has to be tugged to safety. From the computer science perspective, the UAV is performing image processing in order to find the marker marking the object of interest.

III. **Relative distance transmission.** Once the object of interest of within the UAV's field of view, based on the processed image data and altitude information, the UAV transmits the relative distance data to the USV. This data is then used by the USV to perform the *fine approach* manoeuvre.

III. MATHEMATICAL MODELLING

A. The USV model

1) Dynamic model: Following the notation given in [3], dynamic model of the platform in the horizontal plane can be described using the velocity vector $\boldsymbol{\nu} = \begin{bmatrix} u & v & r \end{bmatrix}^{\mathrm{T}}$ where u, v and r are surge, sway and yaw speed, respectively; and the vector of actuating forces and moments acting on the USV $\boldsymbol{\tau} = \begin{bmatrix} X & Y & N \end{bmatrix}^{\mathrm{T}}$ where X, Y are surge and sway forces and N is yaw moment. Both vectors are defined in the body–fixed (mobile) coordinate frame. The uncoupled dynamic model in the horizontal plane is given with (1) where $\mathbf{M}$ is a diagonal matrix with mass and added mass terms, and $\mathbf{D}(\boldsymbol{\nu})$ is a diagonal matrix consisting of nonlinear hydrodynamic damping terms.

$$\mathbf{M}\dot{\boldsymbol{\nu}} = -\mathbf{D}(\boldsymbol{\nu}) + \boldsymbol{\tau} \tag{1}$$

Since the USV is designed to be symmetrical with respect to the x and y axes in the body–fixed frame, hence the matrices $\mathbf{M}$ and $\mathbf{D}$ are diagonal.

2) Kinematic model: The kinematic translatory equations for the USV motion in the horizontal plane is given with (2), where x and y are the position and ψ is the orientation of the platform in the Earth–fixed coordinate frame and $\mathbf{R}(\psi)$ is the rotation matrix.

$$\begin{bmatrix} \dot{x} \\ \dot{y} \end{bmatrix} = \underbrace{\begin{bmatrix} \cos\psi & -\sin\psi \\ \sin\psi & \cos\psi \end{bmatrix}}_{\mathbf{R}(\psi)} \begin{bmatrix} u \\ v \end{bmatrix} \tag{2}$$

Additional equation in the kinematic model is $\dot{\psi} = r$. The USV is overactuated, i.e. it can move in any direction in the horizontal plane by modifying the surge and sway speed, while attaining arbitrary orientation.

B. The dynamic positioning model

By defining the difference between the desired position and the current position in the horizontal plane with

$$\mathbf{e} = \begin{bmatrix} x^* - x \\ y^* - y \end{bmatrix} \tag{3}$$

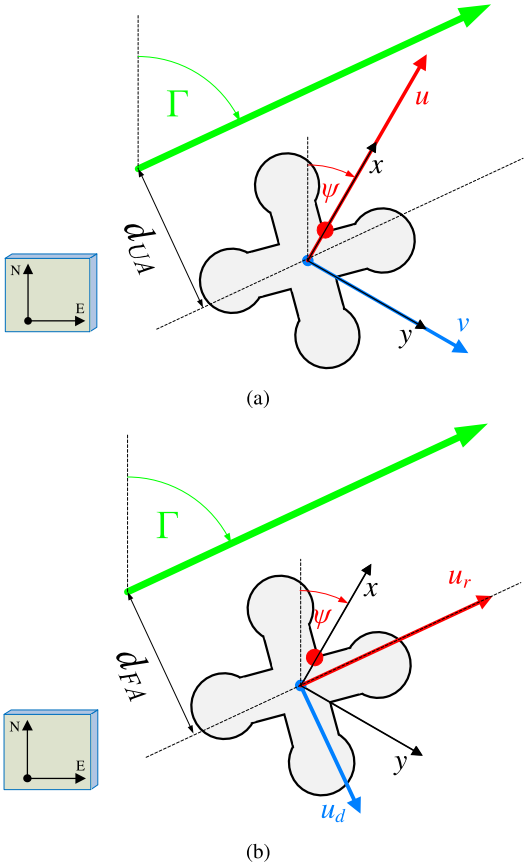

Fig. 2. (a) Underactuated and (b) fully actuated line following.

the kinematic dynamic positioning model can be obtained by differentiation resulting in (4) under the assumption that the desired positions are constant values.

$$\dot{\mathbf{e}} = -\mathbf{R}(\psi) \begin{bmatrix} u \\ v \end{bmatrix} \tag{4}$$

C. Underactuated line following

The underactuated line following approach is shown in Fig. 2(a). The aim is to steer the USV moving at surge speed u in such a way that its path converges to the desired line. If Γ is orientation of the line that should be followed, a new parameter $\beta = \psi - \gamma$ (vehicle's orientation relative to the line) is defined. The kinematic line following equation for underactuated vehicles is then described with (5) and (6), where ξ is drift due to external disturbances which is perpendicular to the direction of the desired path.

$$\dot{\beta} = r \tag{5}$$

$$\dot{d}_{UA} = u\sin\beta + \xi \tag{6}$$

The nonlinear equation (6) can be linearized if angle β is assumed to be small, resulting in $\dot{d}_{UA} = u\beta + \xi$.

D. Fully actuated line following

In the case of fully actuated line following, the vehicle can converge to the desired line while holding an arbitrary

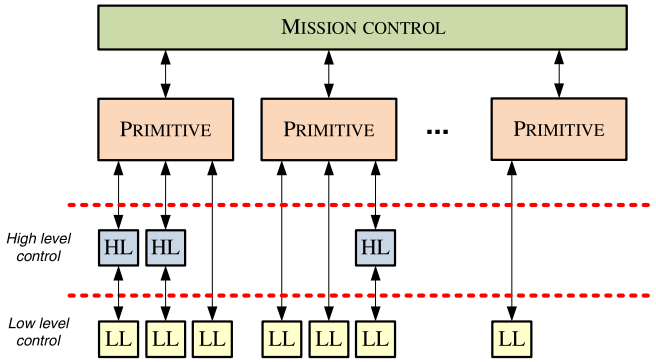

Fig. 3. Generalized control structure divided in mission control, primitives, high–level and low–level controllers.

heading, as it is shown in Fig. 2(b). According to the notation in Fig. 2(b), the kinematic model is given with (7) while u_r and u_d can be calculated using (8). The assumption in this model is that heading ψ is constant during the manoeuvre.

$$\dot{d}_{FA} = u_d + \xi \tag{7}$$

$$\begin{bmatrix} u_r \\ u_d \end{bmatrix} = \begin{bmatrix} \cos(\Gamma - \psi) & \sin(\Gamma - \psi) \\ \sin(\Gamma - \psi) & \cos(\Gamma - \psi) \end{bmatrix} \begin{bmatrix} u \\ v \end{bmatrix} \tag{8}$$

IV. CONTROL STRUCTURE

This section describes the parts of the control structure, shown in Fig. 3, that are required to execute the specific set of tasks described in the previous section, i.e. coarse and fine approach, and tugging. The description is provided in a top–down approach starting with the mission control, primitives, and high and low level controllers.

A. Mission control

We define a mission as a set of primitives that have to be executed. The primitives that comprise a mission are in fact states in a state machine. For the specific mission scenario addressed in this paper, the mission control state machine realized in ROS environments is shown in Fig. 4.

B. Primitives

Primitives are elementary parts that form a mission. They are uniquely defined by the structure of the low–level and/or high–level controllers that they engage, and a set of inputs. As it is shown in Fig. 3, primitives can engage both high–level and low–level controllers. The list of primitives that are used in this paper is given in Table I.

The primitive `go2point_FA` describes the *coarse approach* state of the mission and it engages the high–level heading controller (`heading`) in order to face the platform to the object, and the high–level fully actuated line following controller (`LF_FA`). The first implicitly engages low–level yaw rate controller, while the second implicitly engages the the surge and sway low–level controllers.

The primitive `DP_primitive` describes the *fine approach* state of the mission and it engages the high–level

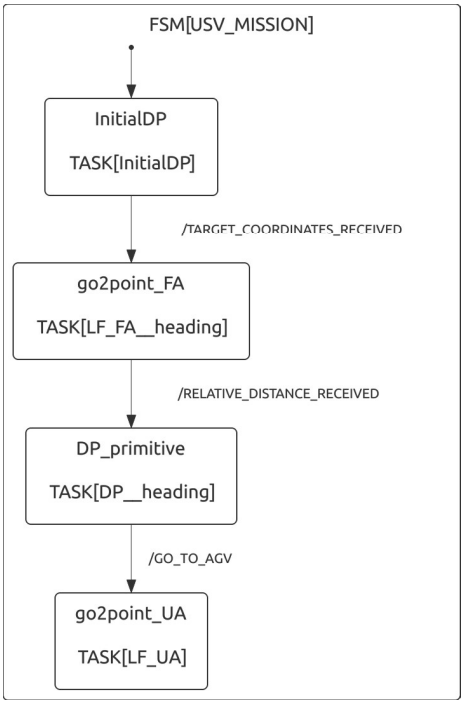

Fig. 4. Mission scenario realized in ROS.

dynamic positioning controller (`DP`) in order to guide the platform closer to the object, and the high–level heading controller with full actuation (`heading`). The first implicitly engages the surge and sway low–level controllers, while the second implicitly engages the low–level yaw rate controller.

The primitive `go2point_UA` describes the *tugging* state of the mission and it engages the high–level underactuated line following controller (`LF_UA`). The heading controller is not engaged since (`LF_UA`) implicitly engages the low–level yaw rate controller which is in charge of the smooth heading transition that will allow keeping the grasp on the object.

The controllers mentioned here are described in the following two subsections.

TABLE I
LIST OF PRIMITIVES.

Name	Inputs	Controllers
`go2point_FA`	T_1, T_2, ψ^*	`LF_FA; heading`
`DP_primitive`	T_1, ψ^*	`DP; heading`
`go2point_UA`	T_1, T_2	`LF_UA`

C. High–level controllers

For the sake of brevity, description of individual controller parameters are omitted. Each controller structure is designed in such a way that convergence of the closed loop is ensured. Controller parameters can be calculated based on the desired closed loop characteristic equation as it is shown in [2].

1) Heading control: The controller generates the desired yaw rate r^* and can be written in the form

$$r^* = -K_{P\psi}(\psi^* - \psi) - K_{I\psi}\int(\psi^* - \psi)\,dt. \tag{9}$$

2) Underactuated line following control: Based on the model given with (5) and (6) the line following controller for underactuated vehicles (or fully actuated vehicles that are required to perform the manoeuver specific to the underactuated vehicles) is given with

$$r^* = -K_{P,d_{UA}} d_{UA} - K_{D,d_{UA}} \dot{d}_{UA}. \qquad (10$$

It should be mentioned that controller parameters depend on the forward speed u of the vehicle, what follows from (6).

3) Fully actuated line following control: Based on the model given with (7) the line following controller for fully actuated vehicles is given with

$$u_d^* = -K_{P,d_{FA}} d_{FA} - K_{I,d_{FA}} \int d_{FA} dt. \qquad (11$$

The desired u^* and v^* can then be calculated using (8).

D. Dynamic positioning (DP) controller

Based on the DP model given with (4), the high–level dynamic positioning controller can be written in the form

$$\begin{bmatrix} u^* \\ v^* \end{bmatrix} = \mathbf{R}^{\mathrm{T}}(\psi) \left(\mathbf{K_{P,DP}} \mathbf{e} + \mathbf{K_{I,DP}} \int \mathbf{e} dt \right) \qquad (12)$$

where $\mathbf{e}$ is given with (3).

E. Low–level controllers

For the low–level speed controller we choose a PI controller in the form

$$\boldsymbol{\tau} = \mathbf{K_{P\nu}} \left(\boldsymbol{\nu}^* - \tilde{\boldsymbol{\nu}} \right) + \mathbf{K_{I\nu}} \int \left(\boldsymbol{\nu}^* - \tilde{\boldsymbol{\nu}} \right) dt + \boldsymbol{\tau_F} \qquad (13)$$

where $\boldsymbol{\nu}^* = \begin{bmatrix} u^* & v^* & r^* \end{bmatrix}^{\mathrm{T}}$ are the desired linear and angular speeds of the platform.The tilde sign marks the estimated values – the vehicle's speeds are often estimated since they are either difficult to measure or are unreliable. The $\boldsymbol{\tau_F}$ term represents additional action introduced in the controller to improve the closed loop behaviour. Most commonly, this is the feedforward action in the form $\boldsymbol{\tau_F} = \mathbf{D}(\boldsymbol{\nu}^*) \boldsymbol{\nu}^*$.

F. Navigation filter

The USV navigation filter is derived from the model given with equations (1) and (2) and it is used to estimate all the states based on the available measurements. During the *coarse approach* phase, when the object is not in the field of view of the daughter UAV, the filter measurement vector consists of GPS and compass measurements, i.e. $y_m = \begin{bmatrix} x & y & \psi \end{bmatrix}$. Once the UAV spots the object, i.e. when the *fine approach* phase is initiated, the measurement vector consist of USV distances relative to the object and the USV orientation from the compass, i.e. $y_m = \begin{bmatrix} \Delta x & \Delta y & \psi \end{bmatrix}$, where $\Delta x = x - x_{object}$ and $\Delta y = y - y_{object}$. Under the assumption that the object is not moving, the same navigation filter structure can be used since $\Delta \dot{x} = \dot{x}$ and $\Delta \dot{y} = \dot{y}$. The only thing that changes is the measurement covariance matrix, due to different measurement sources (GPS and camera).

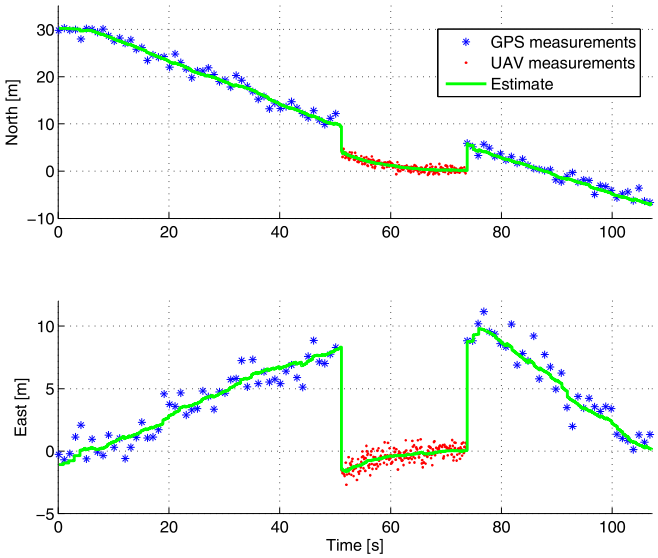

Fig. 5. Measurements and estimates during the three phases of the mission.

V. RESULTS

The simulation results that are presented in this paper demonstrate the three phases of the mission: coarse approach, fine approach and tugging.

Fig. 5 show GPS measurements (blue dots) that were taken as inputs (in the coarse approach and tugging phase), and red dots show the measurements provided by the UAV (relative distance between the USV and the object). Green line shows the estimate from the navigation filter during the whole mission. It is clearly visible that GPS measurements have larger variance in relation to the UAV measurements, and that their sampling rate is lower – 1 Hz in comparison to 10Hz provided by the UAV. The results in this figure demonstrate the functionality of the navigation filter even in cases when the source of measurements is changed.

Fig. 6(a) shows the commanded surge and sway speed (outputs from the high–level controllers) during the three phases of the mission. Fig. 6(b) shows the achieved surge and sway force (output from the low–level controllers). It is obvious that the control structure ensures bumpless transfer between the phases. This is of high importance in order to avoid actuator tear and wear. The only abrupt change in control signal is visible in transition to the final phase of the mission. The reason for this is that during the underactuated line following, surge speed is set to a constant value 0.5m.

The USV trajectory during the mission is shown in Fig. 7. It can be seen that during the *coarse approach* phase (blue line), the USV assumes the required orientation independently of the trajectory. The *fine approach* phase (red line) is initiated once the object (red circle) is in the field of view of the UAV. The *tugging* phase (magenta line) clearly shows the smooth transition to the required line, in order to avoid loosing the grasp of the object.

The video of the mission simulation can be found at [1].

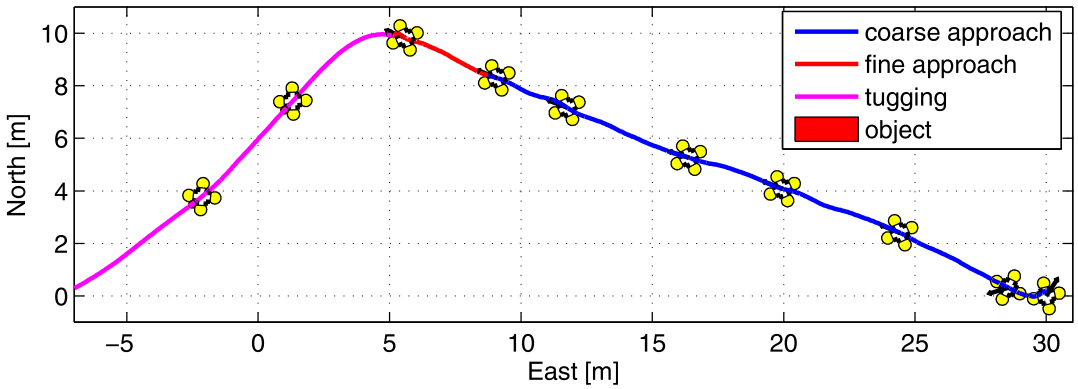

Fig. 7. USV trajectory during the mission.

VI. CONCLUSIONS

This paper presents a simulation of a marsupial system comprising an unmanned surface marine vehicle and an unmanned aerial vehicle. The robotic system was used to execute object recovery from the sea surface. A detailed description of the mission scenario and the control structure developed in ROS is given. Special attention was devoted to mission state switches when navigation measurements are changes from conventional GPS to data provided by the accompanying unmanned aerial vehicle. The results show that the proposed control structure ensures bumpless change in commanded signals when mission states change. The presented results focus on the USV perspective.

Our future research will focus on experimentation with real vehicles, in real–life conditions. The resented results show the applicability of the proposed approach. Even though the simulator realistically models available sensors, it is expected that real–life experiments will require additional effort and modifications.

REFERENCES

[1] http://www.fer.unizg.hr/zari/labust/research/projects/marsupial_robotics.

[2] M. Caccia, M. Bibuli, R. Bono, and G. Bruzzone. Basic navigation, guidance and control of an unmanned surface vehicle. *Autonomous Robots*, 2008.

[3] T.I. Fossen. *Guidance and Control of Ocean Vehicles*. John Wiley & Sons, New York, NY, USA, 1994.

[4] J. Larson, M. Bruch, and J. Ebken. Autonomous navigation and obstacle avoidance for unmanned surface vehicles. volume 6230 I, 2006. cited By (since 1996)6.

[5] M. Lindemuth, R. Murphy, E. Steimle, W. Armitage, K. Dreger, T. Elliot, M. Hall, D. Kalyadin, J. Kramer, M. Palankar, K. Pratt, and C. Griffin. Sea robot-assisted inspection. *Robotics Automation Magazine, IEEE*, 18(2):96–107, June 2011.

[6] N. Miskovic, V. Djapic, D. Nad, and Z. Vukic. Multibeam sonar-based navigation of small uuvs for mcm purposes. volume 18, pages 14754–14759, 2011. cited By (since 1996)0.

[7] N. Miskovic, E. Nad, N. Stilinovic, and Z. Vukic. Guidance and control of an overactuated autonomous surface platform for diver tracking. In *Control Automation (MED), 2013 21st Mediterranean Conference on*, pages 1280–1285, June 2013.

[8] Robin R. Murphy, Michelle Ausmus, Magda Bugajska, Tanya Ellis Tonia Johnson, Tanya Ellis, Tonia Johnson, Nia Kelley, Jodi Kiefer, and Lisa Pollock. Marsupial-like mobile robot societies. In *in Agents 99*, pages 364–365. ACM Press, 1999.

[9] M. Orsag, C.M. Korpela, S. Bogdan, and P.Y. Oh. Hybrid adaptive control for aerial manipulation. *Journal of Intelligent and Robotic Systems: Theory and Applications*, pages 1–15, 2013.

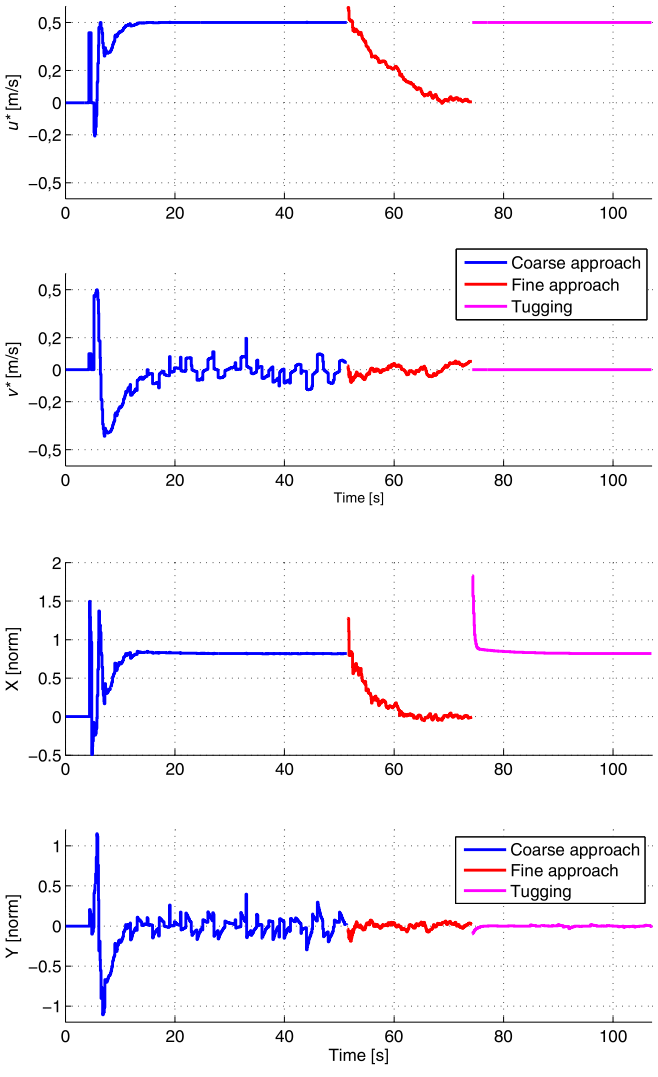

(b)

Fig. 6. (a) Commanded speeds and (b) generated forces during the mission.